

Dyck, H.M. and Milkey, R.W.: 1972, *Publications Astronomical Society of the Pacific* **84**, 597.
 Geisel, S.L.: 1970, *Astrophysical Journal Letters* **161**, L 105.
 Merrill, P.W. and Burwell, C.G.: 1933, *Astrophysical Journal* **78**, 87.
 Ringuelet, A.E., Sahade, J., Rovira, M., Fontenla, J.M. and Kondo, Y.: 1984, *Astronomy and Astrophysics* **131**, 9.
 Sitko, M.L., Savage, B.D., and Meade, M.R.: 1981, *Astrophysical*

Journal **247**, 1024.
 Surdej, J., and Swings, J.-P.: 1976, *Astronomy and Astrophysics* **47**, 113.
 Surdej, J., and Swings, J.-P.: 1977, *Astronomy and Astrophysics* **54**, 219.
 Woolf, N.J., Stein, W.A., and Strittmatter, P.A.: 1970, *Astronomy and Astrophysics* **9**, 252.

Determination of the Rotation Curve of Our Galaxy. Observations of Distant Nebulae

J. Brand, Sterrewacht Leiden, Netherlands

For the derivation of the Galactic gravitational potential, a well calibrated rotation curve of a suitably selected class of objects is a valuable source of information. It gives us insight in problems of galactic dynamics and mass distribution.

This article describes the project currently carried out by the author, in collaboration with Dr. Jan Wouterloot (formerly with ESO) and Dr. Leo Blitz (University of Maryland). Its main purpose is to determine the shape and strength of the gravitational force that influences the motion of material in our Galaxy. We do this by turning our attention to the outer galaxy (third and fourth quadrant), where we try to figure out how the molecular material, and by inference the (young) stars that reside in the disk, moves in those outer reaches of our stellar system. Knowledge of the gravitational potential will give us insight in the way mass is distributed in the Galaxy.

The fact that the Galaxy rotates has been established by Lindblad and Oort in the mid 1920s. The rotation is differential, i.e. the Galaxy does not rotate as a solid disk (as for instance do the wheels of a car, fortunately), but has a different angular velocity at different distances R from the galactic centre (G.C.). Furthermore it is found that different types of objects move in different ways, in the sense that the gas is constrained to move in nearly circular orbits around the G.C., whereas old stars (members of the so-called spheroidal component) move in highly eccentric orbits. The relation that gives the velocity of rotation in circular orbits with respect to the G.C. as a function of distance from the G.C. is called the rotation curve. Ever since the 1920s people have been trying to determine the rotation curve of our galaxy. There are several reasons why this relation is important. Matter in the Galaxy is distributed in a certain way, which determines the shape of the gravitational potential. This potential dictates the orbital parameters of the galactic constituents (stars and gas) and thus the rotation curve that we derive from our measurements of these constituents. Reversing the sequence, the rotation curve tells us how matter in the Galaxy moves and gives clues as to how it is distributed. A practical, and very important, use of a rotation curve is to estimate distances to gas clouds (either HI or HII regions for which the ionizing stars are too much obscured to be seen) by just measuring their velocity.

There are several ways to determine the rotation curve of our Galaxy, depending on the sector of the Galaxy that one investigates. For the inner Galaxy ($l = 90^\circ \rightarrow 0^\circ \rightarrow 270^\circ$) a much used practice is to measure the velocity of the atomic or molecular gas (through respectively the 21 cm line of HI or the 115 GHz (or 230 GHz) line of CO). For a particular line of sight, the emission of the highest-velocity feature is then assigned to the location closest to the G.C., encountered along that line of sight. In this way a rotation curve for the part of the Galaxy inside the solar circle can be constructed. Another way to

reach this goal is to use HII regions and their exciting stars. In that case, the velocities used are that of the ionized gas (e.g. via H α , or H109 α line measurements), of the stars (thought to be) associated with the nebulae, or of the molecular clouds associated with the HII regions. Distances are derived from optical observations (photometry and spectrography) of the exciting stars. Other galactic objects such as Cepheids and planetary nebulae can and have been used as well. From that combined work we now have a fairly good understanding of the rotation characteristics of the inner Milky Way. A disadvantage encountered in the inner Galaxy is that the line of sight samples each radius R twice. This situation is depicted in Fig. 1. Measuring a radial velocity of an object in that part of the Galaxy leaves one in doubt as to whether to assign it to the "near" or "far" distance. One then has to use circumstantial evidence (such as degree of extinction for HII regions or angular sizes of gas clouds in the direction perpendicular to the galactic plane) to solve this dilemma.

For the outer Galaxy ($l = 90^\circ \rightarrow 180^\circ \rightarrow 270^\circ$) things are more straightforward as each velocity corresponds directly to

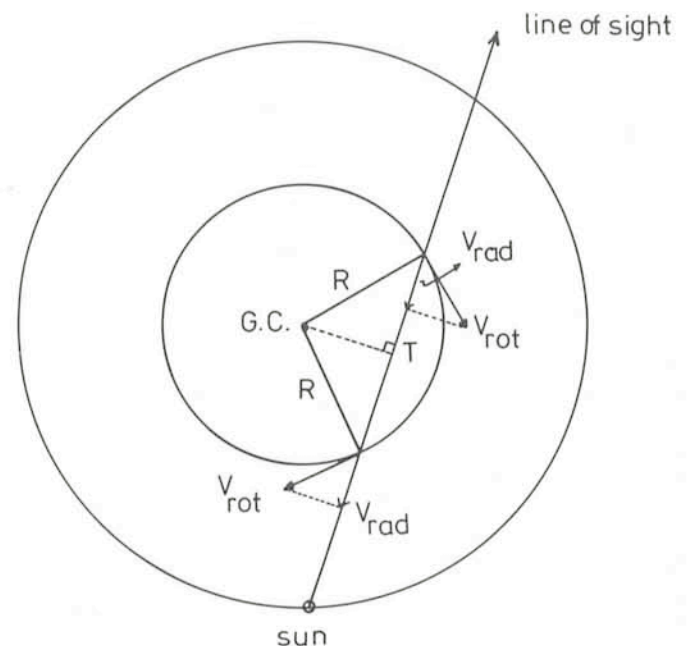


Fig. 1: Distance ambiguity in the inner Galaxy. The line of sight intersects the circle that is the locus of points at a distance R from the G.C. twice. Objects at both intersections have the same velocity. It is assumed that the highest-velocity features along this line of sight are found at point T (= tangential point). V_{rot} and V_{rad} are rotational and radial velocity respectively.

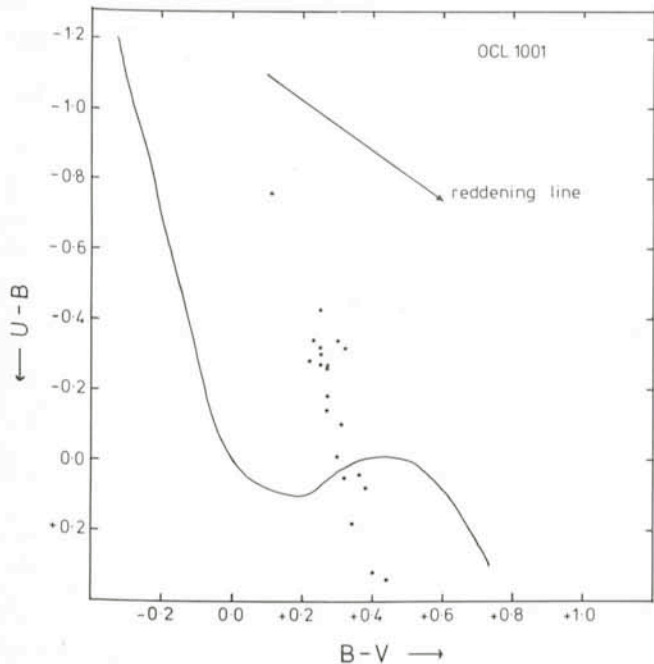


Fig. 2: Colour-colour diagram of the open cluster OCL 1001, constructed from UBV observations with the ESO 1 m telescope. All plotted stars are cluster members. Due to little internal reddening, the points form a sequence parallel to the unreddened ZAMS (drawn curve). The unreddened colours are found by shifting the data points along the reddening line to the ZAMS.

a single distance. There are some other advantages as well, not the least of which is that it is visible from La Silla. In that part of the Galaxy, one can still use H II regions and associated stars and gas to derive the rotation curve. We use the H II itself only as a tracer. It guides us to the stars that we measure to find their distances, and it tells us where the molecular material (invisible to the eye), of which we measure the radial velocity, is to be found. CO surveys have shown that there is not much molecular gas outside the solar circle, so there will be fewer identification problems as to which H II region is associated with which cloud, especially at velocities appreciably different from zero. And finally, related to this, there is a smaller amount of extinction in those parts of the Galaxy than there is in the inner Galaxy, so that we can expect to see quite far out.

The basis of our project are the 600 odd emission objects identified by the author from ESO/SRC survey plates in the region $230^\circ \leq l \leq 305^\circ$, $|b| \leq 10^\circ$. These are either H II regions or reflection nebulae (both types of objects can be used). From the plates we have tried to identify those stars that are likely to be associated with the nebulae (by looking at their position relative to a nebula and signs of interaction, such as bright rims). The first step is then to obtain photometry of those stars. For this we have used the Walraven VBLUW photometer at the Dutch 90 cm and the UBV photometer at the ESO 1 m telescope.

If we plot the colours of the stars of a particular region in a colour-colour diagram (e.g. U-B vs. B-V) and then shift them back, along the reddening line, to the unreddened ZAMS* in that diagram, we obtain the unreddened colours of that star $((U-B)_0$ and $(B-V)_0$) and the colour excess $E(B-V) = (B-V) - (B-V)_0$. From the colours we get an absolute magnitude M_V and from the colour excess we find the visual extinction $A_V = R \times$

* The ZAMS (Zero Age Main Sequence) is the locus of points in the colour-colour diagram on which a star lies at the beginning of its evolution, at the onset of H burning.

$E(B-V)$ ($R \sim 3.2$). We can then derive the stars' heliocentric distance d through the well-known relation $V - M_V = 5 \log d - 5 + A_V$. Using simple geometry, heliocentric distance is converted into galactocentric distance R . When all stars selected are in fact associated with the emission nebula, shifting each star individually will result in the same distance (allowing for some intrinsic spread). Furthermore, if there is no or very little internal reddening in the group, the stars will form a sequence in the colour-colour diagram parallel to the unreddened sequence. This is nicely illustrated in Fig. 2, which gives the observational data of the open cluster OCL 1001 plotted in the (U-B) vs. (B-V) diagram, together with the unreddened ZAMS relation. However, the case is much less clearcut for other objects. This is mostly due to the fact that it is hard to identify possibly associated stars for an H II region so that only some of the selected stars will actually excite the emission region in question. Plotting the data in a colour-colour diagram then gives anything but a nice sequence. This is furthermore complicated by the fact that only stars of luminosity class V should be shifted back to the ZAMS, since stars of other luminosity classes (e.g. Ia (supergiants) or III (giants)) have different unreddened sequences in the diagram. Therefore, knowledge of luminosity class is important. If it is not known, it is relatively safe to assume a luminosity class V for an ionizing star, but a discrepancy in distance between two stars thought to be associated with the same emission region can mean that at least one of the stars is in fact not associated or has a different luminosity class. Therefore, spectra of stars will be taken as well (when this article was written, these observations still had to be done). To illustrate how well this method can work in case we do have knowledge of the luminosity class of the stars, and to show that the distances found are consistent with earlier findings, we have compared in Fig. 3 heliocentric distances derived from the VBLUW data in the way described above, using the published luminosity class, with distances

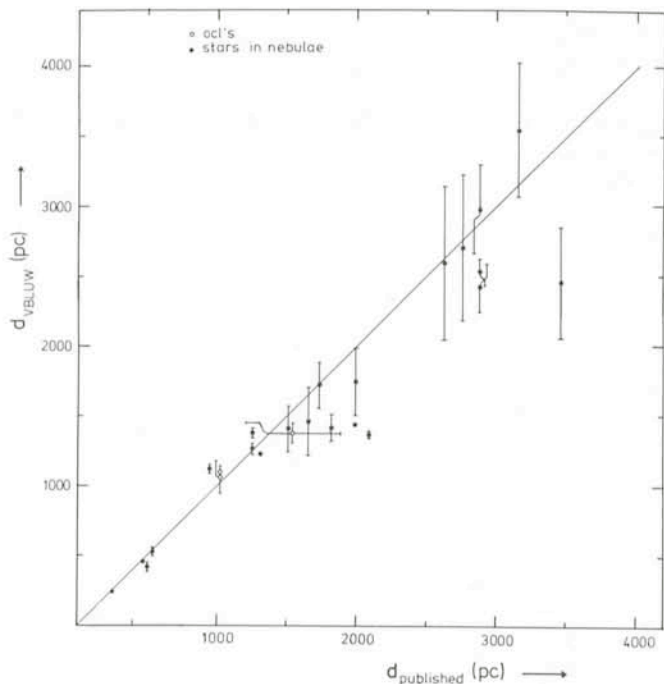


Fig. 3: Comparison of heliocentric distances determined from VBLUW photometry with published distances of the same objects. Plotted points are stars associated with nebulousity and open clusters (in the latter case, average distance of measured member stars is shown). Except for one OCL, no uncertainties are shown for published distances.

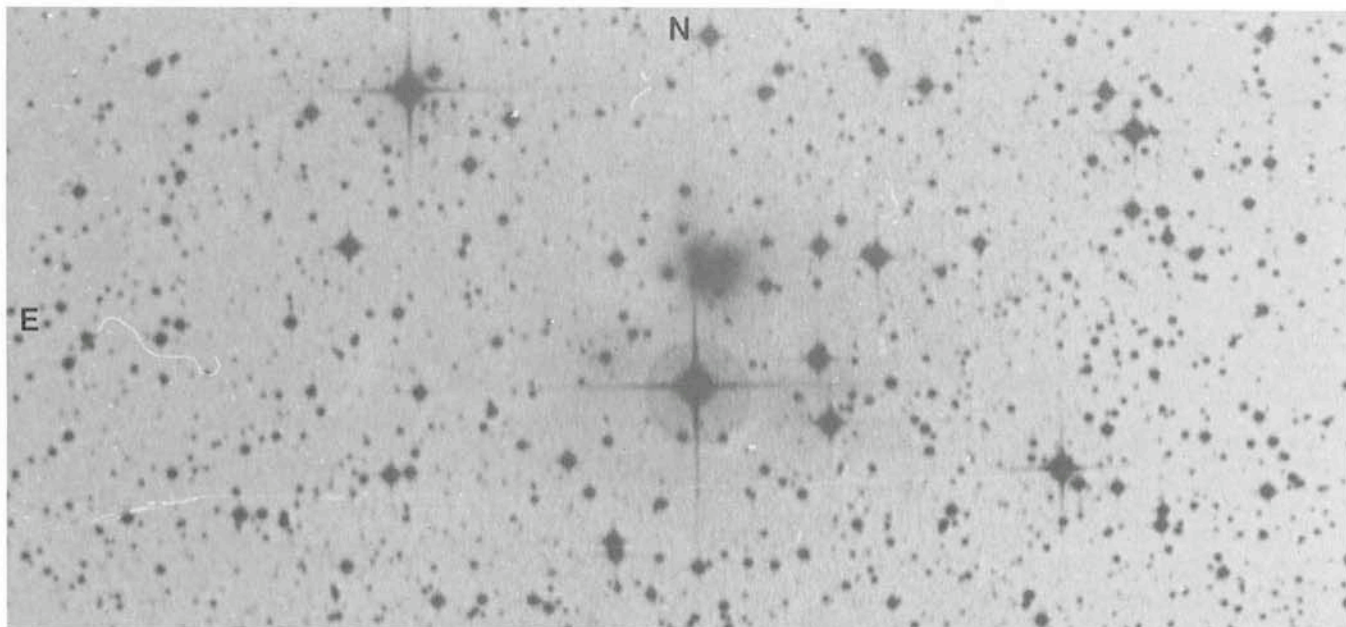


Fig. 4: Example of an emission region in our catalogue with easily identifiable associated stars. In the direction of this region we measure a velocity of 51 km s^{-1} for the CO line. The region is at galactic coordinates $l = 248^\circ$, $b = -5^\circ.5$. Photograph reproduced from ESO/SRC sky survey.

taken from the literature. As we measure five magnitudes in the Walraven system we can construct three independent colour-colour diagrams. The distances shown in Fig. 3 are an average derived from those diagrams.

So much for the way in which the distances are derived. How about the velocities? Half of our total sample of objects was observed with the CSIRO 4 metre dish (Epping, Australia) last year. The remainder will be done later this year. These observations have yielded interesting results in itself. For instance, some line profiles displayed quite broad wings indicating activity in the molecular cloud. Of more concern to the present project, about ten or fifteen clouds near nebulae showed up at velocities in excess of 50 km s^{-1} with respect to the local standard of rest. Examples of such regions are shown in Fig. 4 and 5. A crude indication of the importance of these regions can be given by taking the rotation curve that has been determined by Blitz and co-workers (Blitz, 1979) in similar fashion using the Sharpless HII regions in the second and part of the third quadrant, and substituting the measured radial velocity in a rotation curve equation to get its distance (which is one of the advantages of having a rotation curve at one's disposal, as the reader may recall). With a radial velocity of 77 km s^{-1} , region A of Fig. 5 would be at a distance $R \sim 17$ or 18 kpc from the G. C. From our work so far, and from work done by others in the second galactic quadrant, we infer that it is not very likely that we will find objects very much farther away than this. It seems that what an outside observer would call "the visible disk of the Galaxy" extends at most to about $R = 20 \text{ kpc}$. Even so, as we do not limit ourselves to previously catalogued (and usually relatively nearby) HII regions, we hope (and expect) to find many objects between $R = 15$ and 20 kpc , so that the rotation curve out to that limit can be well determined. Due to the large number of objects in our catalogue, for all of which we can, in principle, determine accurate distances, the errors in the rotation curve will be much smaller than those of previous projects. The stars we think are associated with the nebulae in Fig. 5 are hard to identify (for nebula A) and also too faint ($V \geq 17^m$ for nebula B) for photometry with either the Dutch or the ESO 1 metre telescope. We therefore observed this region (and others like it) with the CCD camera at the new 2.2 metre at La Silla, using B,

V and R filters. In this way we get colours of all stars in the $1'.7 \times 3'.0$ field of view, and down to faint magnitudes (as these data have only been gathered in February 1984, we have not yet been able to reduce them).

We hope to convey the results of our oncoming observing sessions to the reader in a future note to the *Messenger*.

Comments from Tim de Zeeuw and Frank Israel on an earlier version of the manuscript are appreciated.

Reference

Blitz, L., 1979, *Astroph. J. Lett.* **231**, L115.

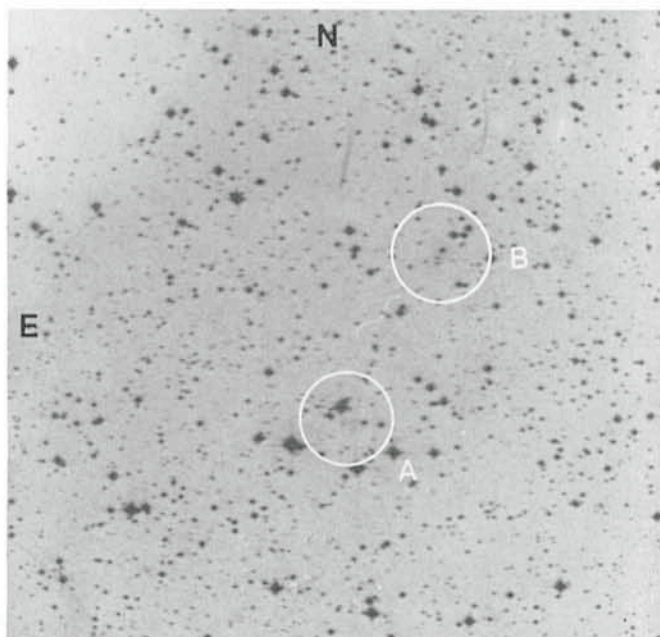


Fig. 5: Example of emission region in our catalogue, associated with molecular material having high radial velocity (reproduction from ESO/SRC sky survey). In the direction of A a CO line at a velocity of 77 km s^{-1} is detected. For B, a line at $V_{\text{LSR}} = 72 \text{ km s}^{-1}$ is measured. Regions A and B are at $l = 237^\circ$, $b = -1^\circ.3$.